Development of a large-scale infiltration column for studying the hydraulic conductivity of unsaturated fouled ballast

Trong Vinh Duong, Viet-Nam Trinh, Yu-Jun Cui, Anh Minh A.M. Tang, Nicolas Calon

Development of a large-scale infiltration column for studying the hydraulic conductivity of unsaturated fouled ballast

Duong T.V.[1], Trinh V.N.[1], Cui Y.J.[1], Tang A.M.[1], Calon N.[2]

1: Ecole des Ponts ParisTech, U.R. Navier/CERMES, 6 – 8 av. Blaise Pascal, Cité Descartes, Champs – sur – Marne, 77455 Marne – la – Vallée cedex 2, France

2: French railway company (SNCF)

Corresponding author:

Prof. Yu-Jun CUI

Ecole des Ponts ParisTech

6-8 av. Blaise Pascal, Cité Descartes, Champs-sur-Marne

F-77455 Marne – la – Vallée cedex - France

Telephone : +33 1 64 15 35 50

Fax : +33 1 64 15 35 62

E-mail : yujun.cui@enpc.fr

Abstract

In order to study the hydraulic behavior of fouled ballast, an infiltration column of 600 mm high and 300 mm in diameter was developed. Five TDR sensors and five tensiometers were installed at various levels, allowing the measurement of volumetric water content and matric suction, respectively. The material studied was fouled ballast that was formed in the railway track-bed by penetration of fine-grained soil into the ballast. This material is characterized by a high contrast of size between the largest and the smallest particles. During the test, three stages were followed: saturation, drainage, and evaporation. Based on the test results, the water retention curve and the unsaturated hydraulic conductivity were determined. The quality of the results shows the capacity of this large-scale infiltration column in studying the unsaturated hydraulic properties of such fouled ballast.

Keywords: Infiltration column; fouled ballast; TDR; tensiometer; water retention curve; hydraulic conductivity.

Introduction

Coarse elements like ballast particles and fine-grained soils co-exist in many geotechnical problems, for instance, in road pavement or railway structures. This is particularly the case for the old railway structures which were initially built by direct emplacement of ballast on sub-soil without separation layer as for the new high-speed lines. After several years of rail traffic, a new layer was developed through the penetration of fine grain soil into the ballast. Sources of fine particles can be train-borne materials (coal, grain, etc), windborne sediments, pumping of subgrade soils, or ballast particle crushing under repeated loading. The phenomenon of filling voids in the ballast layer by fine particles is commonly termed as fouling (Selig and Waters 1994; Indraratna et al. 2011*a*). Indraratna et al. (2011*b*) indicated that highly fouled ballast loses its functions related to water drainage: the permeability of fouled ballast lower than 10^{-4} m/s is considered unacceptable following Selig and Waters (1994). Robinet (2008) investigated the French railway network and observed that 92% of stability problems have been related to insufficient drainage of the platforms. This shows the importance of a good understanding of the hydraulic behavior of soils involved in the platforms, especially fouled ballast.

Up to now, there has been quite limited knowledge on the hydro-mechanical behavior of these kinds of soils, even though it is well recognized that these soils can play an important role in the overall behavior of railway platforms. This is probably due to the difficulty of experimentally working on these coarse-grained soils: common experimental devices for soils can no longer be used and large scale columns are needed. The difficulties are obviously much higher when these soils are unsaturated and their densities are high.

The hydraulic conductivity of saturated soils is mainly a function of their void ratio, while the hydraulic conductivity of unsaturated soils is not only dependent on the void ratio, but also the degree of saturation (or volumetric water content). Nowadays, there are various methods in the literature allowing

62 the determination of unsaturated hydraulic conductivity. Tarantino et al. (2008) described several field
63 techniques to measure suction, volumetric water content and hydraulic conductivity. In the laboratory
64 condition, according to Masrouri et al. (2008), the hydraulic conductivity of an unsaturated soil can be
65 determined using either direct or indirect techniques, based on Darcy's law. According to the flow mode,
66 direct techniques can be divided into steady and unsteady state methods. In the steady state methods, a
67 constant flow rate is needed under a specified average water pressure head. The steady state methods
68 may be costly, tedious and lengthy for low permeability materials. The unsteady state methods are
69 usually divided into two groups: outflow-inflow methods and instantaneous profile methods. In the first
70 group, it is assumed that during the flow process, the hydraulic conductivity is constant and the
71 relationship between water content and matrix suction is linear. The instantaneous profile methods
72 consist of inducing transient flow in a soil specimen and monitoring the water content and suction
73 profiles changes (Wind 1966; Daniel 1982; Delage and Cui 2001; Cui et al. 2008; Ye et al. 2009). When
74 applying this method, very often, only the suction profile is monitored and the water content profile is
75 obtained indirectly based on the water retention curve that is determined separately. Peters et al. (2011)
76 used a fused quartz (transparent soil) with digital image analysis to monitor the degree of saturation
77 during the test, but this method is not suitable for the fouled ballast studied.

78 Infiltration column is usually used to determine the unsaturated hydraulic conductivity of soils
79 following the instantaneous profile method. In most cases, fine-grained soils are studied and the
80 infiltration columns used were of small diameter: for instance, 150 mm by Bruckler et al. (2002),
81 103 mm by Chapuis et al. (2006). Some authors presented larger infiltration columns allowing
82 embedding volumetric water content sensors in addition to suction sensors (Nützmann et al., 1998;
83 Stormont and Anderson, 1999; Choo and Yanful, 2000; Yang et al., 2004; McCartney and Zornberg,
84 2007; McCartney and Zornberg, 2010). In spite of their larger size (diameter around 200 mm), the
85 columns mentioned above are not adapted to coarse-grained soils or fine-coarse grained soil mixtures

where the dimension of the largest particles can reach 60 mm. For these soils, larger infiltration columns are needed. In this regard, Trani and Indraratna (2010) developed a percolation column of 240 mm in diameter and 150 mm in height to investigate the hydraulic behavior of saturated sub-ballast under cyclic loading. The use of large-sized specimens is also specified in the French standard AFNOR (2004): the diameter (D) of the soil specimen for triaxial tests must exceed 5 times the maximum diameter (d_{max}) of soil grains. This size ratio was more or less respected in various works found in literature: Yasuda et al. (1997) conducted triaxial tests with a D/d_{max} equal to 4.7 (D = 300 mm). A ratio of 5.7 was adopted by Lackenby et al. (2007) in their tests on soil specimen of 300 mm in diameter. The same ratio of 5.7 was adopted by Ekblad (2008) with a specimen diameter D equal to 500 mm. It is obvious that the development of such large columns represents a big challenge because of the technically related difficulties. Note that Tang et al. (2009) developed an infiltration tank of rectangular section (800 mm x 1000 mm) with simultaneous suction and volumetric water content monitoring for testing compacted expansive soil. The large size allowed the free swell of soil during wetting but the volumetric sensors used (Thetaprobe) are not suited to the fine-coarse-grained soil mixtures because of the limited dimension of these sensors.

In order to investigate the hydraulic conductivity of fouled ballast in both saturated and unsaturated states, a large-sized infiltration column (300 mm in diameter and 600 mm in height) was developed. This column was equipped with both tensiometers and TDRs allowing the simultaneous monitoring of suction and volumetric water content. Note that the water retention curve can be obtained directly from the measurements, and direct application of the simultaneous method can be done for the determination of the hydraulic conductivity of unsaturated fouled ballast.

Materials

The fouled ballast studied was taken from the sub-structure of an ancient railway at Sénissiat (North West of Lyon, France) that was constructed in the 1800s. This fouled ballast mainly composed of ballast and sub-soil during the degradation of the railway structures. The sub-soil was also taken at this site. Identification tests were performed in the laboratory on these materials. The results show that the sub-soil is high-plasticity silt with a liquid limit w_L = 57.8% and a plasticity index I_p = 24.1. The fraction of particles smaller than 80 µm is 98% and that of particles smaller than 2 µm is 50%. The fouled ballast contains 3% to 10% of stones (50-63 mm), 42% to 48% of ballast (25-50 mm), 36 to 42% of micro-ballast, sand, degraded ballast (0.08 to 25 mm), and 16% fines (<80 µm). It represents a mixture of fine-coarse-grained soils. Figure 1 shows the grain size distribution curves of both the sub-soil and fouled ballast.

The density of particles smaller than 2 mm was determined by the pycnometer method (AFNOR 1991) and a value of ρ_s = 2.67 Mg/m^3 was found. The density of particles larger than 2 mm and those greater than 20 mm was determined using the same method but with a device of larger size (AFNOR 2001): ρ_s = 2.68 Mg/m^3 for both sizes. More details about this fouled ballast can be found in Trinh et al. (2011). The mechanical behavior of this fouled ballast under cyclic loading was investigated by Trinh et al. (2012).

Experimental setup

Figure 2 shows the infiltration column developed to study the hydraulic behavior of the fouled ballast. It has an internal diameter of 300 mm, a wall thickness of 10 mm and a height of 600 mm. The column is equipped with five volumetric water content sensors (TDR1 to TDR5) and five matric suction sensors (T1 to T5) disposed at equal distance along the column (h = 100, 200, 300, 400 and 500 mm). On the top, a hole of 50 mm in diameter was drilled allowing installation of a sensor of suction if needed. A second hole in the center allows water drainage or air expulsion. Two valves are installed at the bottom,

allowing water injection after expulsion of air in the ducts. Two porous stones are placed for the two valves to avoid any clogging of ducts by soil particles. Geotextiles are placed on the top and at the bottom of the soil specimen. O-rings are used to ensure the waterproofness. A Mariotte bottle is used for water injection. As the area occupied by the sensors is just 6.8% of the total apparatus section area, the sensors installation is expected to not affect the water transfer inside the soil column.

The TDR probes used are of waveguides buried (GOE) type, with 3 rods of 3.2 mm diameter and 200 mm length. According to Soilmoisture (2000), the influence zone of this TDR is 20-30 mm around the rods. The accuracy of the TDR probes is ± 2% of the measured values following the provider. The equipments used (TDR probe and Trase BE) can automatically provide the dielectric constant K_a (which is deduced from the crossing time of electric wave within the surrounding material). Based on the calibration curve (relationship between the dielectric constant and volumetric water content) provided by the producer, the volumetric water content can be then determined. It is thereby an indirect measurement method. Several authors have shown that the calibration curve depends on the texture, density, mineralogical composition, fines content and particle size of the test material (Jacobsen and Schjønning 1993; Stolte et al. 1994; Côté and Roy 1998; Hanson and Peters 2000; Gong et al. 2003; Schneider and Fratta 2009; Ekblad and Isacsson 2007). It is therefore necessary to determine the specific calibration curve for each soil studied. Soil matric suction was measured by T8 tensiometer (UMS 2008). The working pressure range of those tensiometers is from 100 kPa to -80 kPa (they measure both positive pressure and suction), with an accuracy of ± 0.5 kPa.

Experimental procedure

The soil studied was firstly dried in an oven at 50°C for 24 h. Water was then added using a large mixer to reach the target water content. After mixing, the wet material was stored in hermetic containers for at least 24 h for moisture homogenization.

The soil specimen was then prepared by compaction in six layers of 0.10 m each in the infiltration column using a vibrating hammer. The density of each layer was controlled by fixing the soil weight and the layer height. Before compaction of the subsequent layer, a TDR probe and a metal rod of 25 mm diameter were placed on the compacted layer. Once the soil specimen was prepared, the metal rods were removed to install the tensiometers. This protocol was adopted because the tensiometers are fragile and they can't stand the compaction force without being damaged. Considering the influence zone of TDR probes, the distance between the tips of tensiometers and TDR probes was set greater than 40 mm. In order to ensure the good contact between tensiometers and soil, a paste made of sub-soil was injected in the holes before introducing the tensiometers.

The test was carried out in 3 stages: saturation, drainage and evaporation. The specimen was saturated by injecting water from the bottom. Water was observed at the outlet in less than one hour, and the soil specimen was considered saturated after one day of water flow. Saturated hydraulic conductivity was measured by applying a constant hydraulic head of 0.45 m, using the Mariotte bottle. After completion of the saturation, tensiometers were installed on the column. Note that these sensors were not installed before the saturation stage in order to avoid any cavitations due to possible high suctions in the compacted material. After the installation of tensiometer, the soil column was re-saturated again because the soil was de-saturated when installing the tensiometers. After the saturation stage, water was allowed to flow out through the two bottom valves. After two days, when there was no more water outgoing, it was considered that the drainage stage was completed. The top cover of the column was then removed to allow evaporation. The two bottom valves were closed during this stage. The air conditions in the laboratory during this stage were: a temperature of 22°C and a relative humidity of 50±5%. The evaporation ended after about 160 h when the value given by the tensiometer T5 (h = 500mm) was -50 to -60 kPa.

Calibration of the TDR was performed within the same soil specimen. After re-saturating the soil inside the column, drainage was performed step-by-step. The drainage valve was opened to let 300 mL of water drained, and then closed again until reaching the equilibrium of the TDR measurement inside the column. This drainage was then repeated 10 times until the full drainage of pore-water inside the soil specimen. For each step, as the TDR measurement reached the equilibrium, hydrostatic water pressure distribution can be expected and the water content can then be estimated for each level of soil column based on the quantity of water drained. These values of water content were then plotted versus the value of K_a given by the TDR in order to determine the calibration curve (Figure 3). The following equation can be then used for the calibration curve of the TDR:

$$\theta_{cal} = 0.0221 \times K^2_a + 0.5118 \times K_a - 3.0677 \quad (1)$$

Experimental results

The soil was compacted in the infiltration column at a density of 2.01 Mg/m^3 (a porosity of 0.25) and a gravimetric water content of 5.5 %, corresponding to a volumetric water content of 10%. Figure 4 shows the measured volumetric water content by TDR probes after compaction (initial state). These values are respectively 4.8, 6.0, 9.7, 8.8 and 10.1% for TDR1 to TDR5. At t = 80 h, water was injected from the base of the column to saturate the soil. It can be observed that the measured volumetric water content by TDR probes increased quickly and reached a maximum value in less than one hour. The maximum values were 23.4, 23.7, 24.4, 22.4 and 25.0% for TDR5 to TDR1, respectively. Note that at a dry density of 2.01 Mg/m^3, the volumetric water content in saturated state was 25.0%. These values corresponded to a degree of saturation of 93.6, 94.8, 97.6, 89.6 and 100%, respectively, indicating that the specimen was close to the saturated state.

198 The volume of water injected during the saturation stage is shown in Figure 5. In the beginning,
199 the volume of water increased quickly and the rate decreased with time. Note that after t = 50 min, water
200 was observed on the surface of the specimen. The volume of water injected for that time was 4.000×10^{-3}
201 m^3, while that required to saturate the specimen was 5.795×10^{-3} m^3 (calculated from the density and the
202 initial water content of the specimen). The average degree of saturation at this time was then about 70%.
203 From t = 50 min, the relationship between volume of water and time was almost linear. Two tests for
204 measuring hydraulic conductivity at saturated state were performed, 1 day and 3 days respectively after
205 the saturation stage; this delay allowed improving the saturation of the soil. Figure 5 shows that the
206 water volume rates of the two tests are similar. The average value of the hydraulic conductivity
207 estimated is 1.75×10^{-5} m/s.

208 When the specimen was re-saturated, the level of the water surface was maintained at 10 mm
209 above the surface of the specimen. The water pressure values of T1 to T5 were respectively 5.1, 4.1, 3.1,
210 2.1 and 1.2 kPa (Figure 6a) corresponding to water levels of 510, 410, 310, 210 and 120 mm,
211 respectively. This was consistent with the positions of the tensiometers. In the drainage stage, the water
212 pressure decreased. The values became negative five minutes after opening the valves. Then, the
213 changes followed a constant rate for each tensiometer. All tensiometers except T2 (h = 200mm)
214 indicated a lower pressure (higher suction) at a greater elevation (closer position to the evaporation
215 surface).

216 With the same time reference, Figure 6b shows the responses of the five TDR sensors. The
217 responses in volumetric water content were similar to that in water pressure, i.e., the volumetric water
218 content decreased quickly from the maximum value in 10 min. At t = 90 min, the measured volumetric
219 water content ranged from 15 to 17% except that by TDR2 (12%).

The drainage stage was maintained for 54 h and the water pressure responses are shown in Figure 7a. The drainage stage stopped when no more water outflow was observed from the bottom valves (t = 54 h). The measured pressures were -2.0, -1.9, -1.6, -1.8 and -2.7 kPa for tensiometers T1 to T5, respectively. Figure 7b shows the responses of the five TDR probes. At the end of the drainage stage (t = 54 h), the volumetric water contents were 11.7, 7.9, 11.8, 10.8 and 10.9% for TDR1 to TDR5, respectively. It can be seen that both the water pressure and volumetric water content did not reach equilibrium.

After the drainage stage, the bottom valves were closed, and evaporation was allowed from the top side for 160 h. Figure 8a shows the water pressure changes. The tensiometer close to the surface (T5) shows that the pressure decreased quickly from -2.7 kPa to -61.2 kPa after 160 h of evaporation, while those of other levels decreased much more slowly. The value at h = 100 mm remained almost unchanged, around -2.0 kPa.

The values of water content are shown in Figure 8b. Due to a technical problem, data are only available for t = 0-120 h. The same trends as for water pressure changes can be observed: the closer the tensiometer to the evaporation surface, the larger the volumetric water content changes. The value at h = 500 mm (the closest tensiometer to the evaporation surface) decreased from 11% to 7% after 120 h, while those at h = 100 mm and 200 mm remained almost constant.

Determination of the hydraulic properties in unsaturated state

As mentioned before, unlike the common infiltration column with only suction profile monitoring (Daniel 1982; Cui et al. 2008; Ye et al. 2009) or only water content monitoring, the column developed in this study is equipped with both tensiometers and TDR sensors, allowing simultaneous measurements of suction and volumetric water content at different levels. The simultaneous profile method can be then directly applied without using the water retention curve. Before determining the

243 unsaturated hydraulic conductivity of the soil, as one of the important hydraulic properties, the water
244 retention curve (WRC) was determined based on the measurements of suction and volumetric water
245 content during the test. In Figure 9 the measured volumetric water content is plotted versus the measured
246 suction for each level. Except the data at h = 200 mm, the water retention curves obtained for various
247 depth were similar. The best fit curves obtained from the models of van Genuchten (van Genuchten
248 1980) and Brooks-Corey (Brooks and Corey 1964; Stankovich and Lockington 1995) are also shown.
249 The models formula and parameters are presented in Table 1.

250 Figure 10a shows the values of suction isochrones obtained during the evaporation stage. At the
251 beginning (t = 0), suction in the soil was similar and quite low (lower than 2 kPa), then it increased at
252 different rates depending on the position. The closer the tensiometer to the evaporation surface the faster
253 the suction changes. These suction isochrones were used to determine the slope of the total hydraulic
254 head which was in turn used to calculate the hydraulic gradient ($i = \partial h/\partial z$). The measured volumetric
255 water content isochrones are shown in Figure 10b. The isochrones of calculated volumetric water
256 content from the suction measured using van Genuchten's equation (Table 1) are shown in Figure 10c,
257 together with the water content profile at the end of the saturation stage. A general decrease during the
258 evaporation is observed: the curves are shifting leftwards especially for the upper part close to the
259 evaporation surface.

260 McCartney et al. (2007) observed that small variations of suction or volumetric water content in
261 experimental data can result in significant error in hydraulic conductivity. In the present study, the
262 calculation of unsaturated hydraulic conductivity was performed using both the measured water content
263 data (Figure 10*b*) and the calculated results (Figure 10*c*), together with the suction profiles (Figure 10*a*)
264 of the evaporation state. The volume of water passing through a given height for two different times was
265 determined based on the isochrones of volumetric water content. This volume was used to determine the
266 flow rate *q*. The hydraulic conductivity was calculated using Darcy's law. In the calculation of water

volume, three different heights (h = 400, 450 and 500mm) were considered. This calculation was relatively easy with the volumetric profiles shown in Figure 10*c*, but a little difficult for that shown in Figure 10*b* when considering the height lower than h = 300 mm. Indeed, Figure 10*b* shows that negative values can be obtained when determining the water volume passing through the height h = 300 mm. This is mainly because of the little changes in this zone and the accuracy of the measurements. In the calculation, the non physical negative values were not considered for the determination of hydraulic conductivity. Figure 11 shows the relationship between the hydraulic conductivity of soil at a dry density ρ_d = 2.01 Mg/m^3 and suction, obtained using both Figure 10*b* and Figure 10*c*. It can be observed that the two types of volumetric water content profiles gave similar results. A general decrease with increasing suction is observed for the hydraulic conductivity. In this figure the value obtained during the saturation stage is also shown. From the saturated state to an unsaturated state at a suction of 65 kPa, the hydraulic conductivity decreased from 1.75×10^{-5} m/s to 2×10^{-10} m/s.

Figure 12*a* shows the comparison between the determined hydraulic conductivity and the values calculated from the van Genuchten's model and Brooks-Corey's model. Note that the same parameters as for the water retention curve were used when applying these two models. A general lower hydraulic conductivity was given by the models, especially by the van Genuchten's model. A better agreement between the determined and calculated values (Figure 12*b*) can be obtained using the models parameters in Table 1. Similar observation was made by Parks et al (2012): the van Genuchten's model, within parameters obtained when fitting the water retention curve, does not provide an adequate prediction of the experimental hydraulic conductivity functions of unsaturated soils in general.

Discussion

The dry density of the soil studied is as high as 2.01 Mg/m^3. Heavy compaction was needed to reach it. To avoid damage of the tensiometers, metallic rods were used to prepare spaces during compaction for

tensiometers installation. For TDR sensors, they were placed between different soil layers and were compacted together with the soil. The good response of these sensors during the test shows that they were not damaged by the compaction. The inconsistent data given by the TDR sensor at h = 200 mm (see Figure 4) is rather related to the soil heterogeneity. This observation confirms the difficulty of preparing large-size specimen of fined-coarse grained soils on the one hand, and on the other hand, the necessity of using representative large-size specimen for the investigation of hydraulic behavior of such materials. In figure 9, it was noted that a volumetric water content of 5% corresponds to a degree of saturation of 20%. This can be explained by the presence of the large particles of ballast in the soil.

During injection of water, there was a difference between the estimated pore volume and the volume of water injected to reach saturation (Figure 5). This can be explained by the non-uniform flow in the specimen because water flows mainly through the macro-pores. This phenomenon was also reported by Moulton (1980). This means that water outflow from the top valve is not an indicator of full specimen saturation, and longer flow duration is needed (one day in this study). The values of degree of saturation measured by TDR sensors were in the range between 90% and 100% after this stage (see Figure 10*b*).

In the present work, the hydraulic conductivity of unsaturated fouled ballast was obtained in the infiltration column during the drainage and evaporation stages. Following ASTM (2010), the hydraulic conductivity of unsaturated soils can be estimated from infiltration column test following four methods: downward infiltration of water onto the surface of an initially unsaturated soil specimen (A1), upward imbibitions of water from the base of an initially unsaturated soil specimen (A2), downward drainage of water from an initially saturated soil specimen (A3), and evaporation of water from an initially saturated soil specimen (A4). Methods A1 and A2 can be used for fine-grained sands and for low-plasticity silts. Method A3 can be used with fine or coarse-grained sands. Method A4 can be used for any soil with the exception of clays of high plasticity. In the work of Moore (1939), unsaturated flow was induced

naturally; the water rose from the water table to the surface of the soil column and was evaporated from the surface. This method allowed studying various soils ranging from fine gravel to clay.

In the saturated condition, the hydraulic conductivity obtained in the saturated condition is 1.75×10^{-5} m/s. According to the classification of Bear (1988) for railway application, the drainage is poor because this value corresponds to the hydraulic conductivity of very fine sand, silt, or loam. Note that in the material studied, there are also clay (5%), fine sand and loam. Thus, from a practical point of view, this soil cannot be used for drainage layer.

Conclusions

A large scale infiltration column was developed to study the hydraulic behavior of a fine-coarse grained mixture from the fouled ballast layer of a railway constructed in the 1800s. The column is equipped with tensiometer and TDRs to monitor the matric suction and volumetric water content, respectively. The results obtained allow the following conclusions to be drawn:

The quality of the recorded responses show that the installation protocol adopted for tensiometer probes (using metallic rod) and TDR probes (compacted together with soil) was appropriate when testing fine-coarse-grained soils such as the fouled ballast. In addition, the use of both tensiometer and TDR probes in the test enabled the direct determination of water retention curve and the direct application of the instantaneous method for determining the hydraulic conductivity of the unsaturated soil. The results of hydraulic conductivity obtained by both the measured volumetric water content profiles and those fitted using the van Genuchten's model were found similar. This indicates that fitting curves can be used when determining the hydraulic conductivity of unsaturated fouled ballast without causing significant error.

From a practical point of views, the method developed in this study can be used in determining the hydraulic conductivity for fouled ballast in particular and for fine-coarse-grained soil mixtures in general, in both unsaturated and saturated states.

Acknowledgement

This study was carried out within the research project "Track substructure without drainage - permeable structure". The authors would like to thank Ecole des Ponts ParisTech (ENPC), Railway Network of France (RFF) and French Railways Company (SNCF) for their supports. The authors address equally their deep thanks to the French National Research Agency for funding the present study which is part of the project - RUFEX "Reuse of existing foundations".

References:

ASTM, 2010, "Standard test methods for measurement of hydraulic conductivity of unsaturated soils," D7664-10.

AFNOR, 1991, "Soils : investigation and testing – Determination of particle density – Pycnometer method," *French standard*, NF P 94-054.

AFNOR, 2001, "Tests for mechanical and physical properties of aggregates. Part 6: Determination of particle density and water absorption," *French standard*, NF EN 1097-6.

AFNOR, 2004, "Unbound and hydraulically bound mixtures. Part 7: cyclic load triaxial test for unbound mixtures," *French standard*, NF EN 13286-7.

Bear, J., 1988, "Dynamic of fluids in porous media," *Dover Publications*, 781 p.

354 Brooks, R.H., and Corey, A.T., 1964, "Hydraulic properties of porous media", Hydro. Paper No.3,
355 Colorado State Univ., Fort Collins, Colo.

356 Bruckler, L.B., Angulo-Jaramillo, P., Ruy, R., 2002, "Testing an infiltration method for estimating soil
357 hydraulic properties in the laboratory," *Soil Science Society of America Journal*, Vol. 66, pp. 384–395.

358 Chapuis, R.P., Masse, I. , Madinier, B., Aubertin, M., 2006, "Essai de drainage en colonne pour obtenir
359 les propriétés non saturées de matériaux grossiers," *Sea to Sky Geotechnique – the 59th Canadian*
360 *Geotechnical Conference*, pp. 905 – 912.

361 Choo, L.-P., and Yanful, E.K., 2000, "Water flow through cover soils using modeling and experimental
362 methods," *Journal of Geotechnical and Geoenvironmental Engineering*, Vol. 126, No. 4, pp. 324-334.

363 Côté, J., and Roy, M., 1998, "Conductivité hydraulique de matériaux de fondations de chaussées
364 partiellement saturés," *Rapport de l'études et recherches en transports du Québec*, 177 p

365 Cui, Y.J., Tang, A.M., Loiseau, C., Delage, P., 2008, "Determining the unsaturated hydraulic
366 conductivity of a compacted sand-bentonite mixture under constant-volume and free-swell conditions,"
367 *Physics and Chemistry of the Earth, Parts A/B/C*, Vol. 33, pp. S462–S471.

368 Daniel, D.E., 1982, "Measurement of hydraulic conductivity of unsaturated soils with thermocouple
369 psychometers," *Soil Science Society of Americal Journal*, Vol. 46, No. 6, pp. 1125-1129.

370 Delage, P., and Cui, Y.J., 2001, "Comportement mécanique des sols non saturés," *Ed. Techniques*
371 *Ingénieur*, Article C 302.

372 Ekblad, J., 2008, "Statistical evaluation of resilient models characterizing coarse granular materials,"
373 *Materials and Structures*, Vol. 41, No. 3, pp. 509–525.

Ekblad, J., and Isacsson, U., 2007, "Time-domain reflectometry measurements and soil-water characteristic curves of coarse granular materials used in road pavements," *Canadian Geotechnical Journal*, Vol. 44, No. 7, pp. 858–872.

Gong, Y., Cao, Q., and Sun, Z., 2003 "The effects of soil bulk density, clay content and temperature on soil water content measurement using time-domain reflectometry," *Hydrological Processes*, Vol. 17, No. 18, pp. 3601–3614.

Hanson, B., and Peters, D., 2000, "Soil type affects accuracy of dielectric moisture sensors," *California Agriculture*, Vol. 54, No. 3, pp. 43–47.

Indraratna, B., Su, L. and Rujikiatkamjorn, C., 2011*a*, "A new parameter for classification and evaluation of railway ballast fouling," *Canadian Geotechnical Journal,* Vol. 48, No. 2, pp. 322–326.

Indraratna, B., Salim, W. and Rujikiatkamjorn, C., 2011*b*. "Advanced Rail Geotechnology - Ballasted Track," *CRC Press*.

Jacobsen, O.H., and Schjønning, P., 1993, "A laboratory calibration of time domain reflectometry for soil water measurement including effects of bulk density and texture," *Journal of Hydrology*, Vol. 151, No. 2-4, pp.147–157.

Lackenby, J., Indraratna, B., Mcdowell, G., and Christie, D., 2007, "Effect of confining pressure on ballast degradation and deformation under cyclic triaxial loading," *Géotechnique*, Vol. 57, No. 6, pp. 527 – 536.

Masrouri, F., Bicalho, K.V., and Kawai,K., 2008, "Laboratory hydraulic testing in unsaturated soils," *Geotechnical and Geological Engineering*, Vol. 26, No. 6, pp. 691–704.

McCartney, J.S., Villar, L.F.S., and Zornberg, J.G., 2007, "Estimation of the hydraulic conductivity of unsaturated clays using infiltration column test," *Proceedings of the 6th Brazilian Symposium on Unsaturated Soils*, Vol. 1, pp. 321-328.

McCartney, J.S. and Zornberg, J.G., 2007, "Effect of wet-dry cycles on capillary break formation in geosynthetic drainage layers," *Geosynthetics 2007*, Washington, DC. January, pp. 16-19.

McCartney, J.S. and Zornberg, J.G., 2010, "Effect of infiltration and evaporation on geosynthethic capillary barrier performance," *Canadian Geotechnical Journal*, Vol. 47, No. 11, pp. 1201-1213.

Moulton, L.K., 1980, "Highway subdrainage design," *Report to the Federal Highway Administration – U.S. Departement of Transport*, FHWA-TS-80-224, 162 p.

Moore, R., 1939, "Water Conduction from Shallow Water Tables," *Hilgardia*, Vol. 12, pp. 383-426.

Nützmann, G., Thiele, M.,Maciejewski, S. and Joswig, K., 1998, "Inverse Modelling techniques for determininghydraulic properties of coarse-texturedporous media by transient outflow methods," *Advance in Water Resources. Vol. 22, No. 3, pp.273-284.*

Parks, J.M., Stewart, M.A., and McCartney, J.S., 2012, "Validation of a Centrifuge Permeameter for Investigation of Transient Infiltration and Drainage Flow Processes in Unsaturated Soils", *Geotechnical Testing Journal*, Vol. 35, No. 1. pp. 182-192.

Peters, S.B., Siemens, G., and Take, W.A., 2011, "Characterization of transparent soil for unsaturated applications," *Geotechnical Testing Journal*, Vol 34, No. 1, pp. 445-456.

Robinet, A., 2008, "Les couches de forme traitées dans les structures d'assise ferroviaires." *Mémoire de diplôme d'ingénieur du Conservatoire National des Arts et Métiers (CNAM).*

414 Schneider, J.M., and Fratta,D., 2009, "Time-domain reflectometry - parametric study for the evaluation
415 of physical properties in soils," *Canadian Geotechnical Journal*, Vol. 46, pp. 753–767.

416 Selig, E. and Waters, J., 1994, "Track geotechnology and substructure management," *Thomas Telford*.

417 Soilmoisture, 2000, "6050X3K1 Operating Instructions", 53 p.

418 Stankovich, J. M., and Lockington, D. A., 1995, "Brooks-Corey and van Genuchten, soil-water-retention
419 models" *Journal of Irrigation and Drainage Engineering*, Vol. 121, No. 1, 7 pages.

420 Stormont, J.C., and Anderson, C.E., 1999, "Capillary barrier effect from equilibrium technique at
421 different temperatures and its application in determining the water retention properties of MX80 clay,"
422 *Canadian Geotechnical Journal*, Vol. 42, No. 1, pp. 287-296.

423 Stolte, J., Veerman, M ., Wosten, G.J., Freijer, J.H.M., Bouten, J.I ., Dirksen, W., Van Dam, C., Van den
424 Berg, J.C., 1994, "Comparison of six methods to determine unsaturated soil hydraulic conductivity," *Soil*
425 *Science Society of America Journal*, Vol. 58, No. 6, pp. 1596-1603.

426 Tang, A.M., Ta, A.N., Cui, Y.J., and Thiriat., J., 2009, "Development of a large scale infiltration tank
427 for determination of the hydraulic properties of expansive clays," *Geotechnical Testing Journal*, Vol. 32,
428 pp. 385-396.

429 Tarantino, A., Ridley, A.M., and Toll. D.G., 2008, "Field measurement of suction, water content, and
430 water permeability," *Geotechnical and Geological Engineering*, Vol. 26, No. 6, pp. 751–782.

431 Trani, L. D. O., and Indraratna. B., 2010, "Assessment of subballast filtration under cyclic loading,"
432 *Journal of Geotechnical and Geoenvironmental Engineering*, Vol. 136, No. 11, pp. 1519–1527.

433 Trinh, V.N., Tang, A.M., Cui, Y.J., Dupla, J.C., Canou, J., Calon, N., Lambert, L., Robinet, A., and
434 Schoen, O., 2011, "Caractérisation des matériaux constitutifs de plate-forme ferroviaire ancienne,"
435 *Revue Française de Géotechnique*. No. 134-135., pp. 64-75.

436 Trinh V.N., Tang A.M., Cui Y.J., Dupla J.C., Canou J., Calon N., Lambert L., Robinet A., Schoen O.
437 2012, "Mechanical characterisation of the fouled ballast in ancient railway track substructure by large-
438 scale triaxial tests," *Soils and Foundations*. Accepted for publication.

439 UMS, 2008, "T8-long-term monitoring tensiometer," *User manual*, 56 pages.

440 van Genuchten, M.T., 1980, "A closed-form equation for predicting the hydraulic conductivity of
441 unsaturated soils," *Soil Science Society of America Journal*, Vol. 44, No. 5, pp. 892–898.

442 Wind, G.P., 1966 "Capillary conductivity data estimated by a simple method," *In* "Water in the saturated
443 zone," *Proceedings of the Wageningen symposium,*Wageningen, the Netherlands, 19–23 June 1966, pp.
444 181 – 191.

445 Yang, H., Rahardjo, H., Wibawa, B., and Leong, E.C., 2004, "A soil column apparatus for laboratory
446 infiltration study," *Geotechnical Testing Journal*, Vol. 27, pp. 347-355.

447 Yasuda, N., Matsumoto, N., Yoshioka, R., and Takahashi, M., 1997, "Undrained monotonic and cyclic
448 strength of compacted rockfill material from triaxial and torsional simple shear tests," *Canadian*
449 *Geotechnical Journal*, Vol. 34, No. 3, pp. 357-367.

450 Ye W.M., Cui Y.J., Qian L.X., Chen B. 2009. "An experimental study of the water transfer through
451 compacted GMZ bentonite," *Engineering Geology*, Vol. 108, pp.169- 176.
452

Table 1: Model formula and parameters (θ: volumetric water content, θ_r: residual volumetric water content; θ_s: volumetric water content at saturated state; k: hydraulic conductivity; k_s: hydraulic conductivity at saturated state; ψ: suction in kPa; ψ_a: air entry value; α, n, m, and λ are constants).

Model	Formula	Parameters for water retention curve	Parameters for hydraulic conductivity
van Genuchten	$\theta = \theta_r + \frac{\theta_s - \theta_r}{\left[1+(\alpha\psi)^n\right]^m}$ $k = k_s \Theta^2 \left[1-\left(1-\Theta^{1/m}\right)^m\right]$ $with: \Theta = \frac{\theta - \theta_r}{\theta_s - \theta_r}$	θ_s = 25.0% θ_r = 0% α = 0.4 kPa^{-1} ; n = 1.17 ; m = 0.15	θ_s = 25.0 % θ_r = 0 % m = 0.2
Brooks-Corey	$\theta = \theta_s$ *if* $\psi < \psi_a$ $\theta = \theta_s \left(\frac{\psi_a}{\psi}\right)^{\lambda}$ *if* $\psi \geq \psi_a$ $k = k_s \left(\frac{\psi_a}{\psi}\right)^{2+3\lambda}$	θ_s = 25.0% ψ_a = 0.02 kPa λ = 0.17	ψ_a = 0.1 kPa λ = 0.01

List of Figures

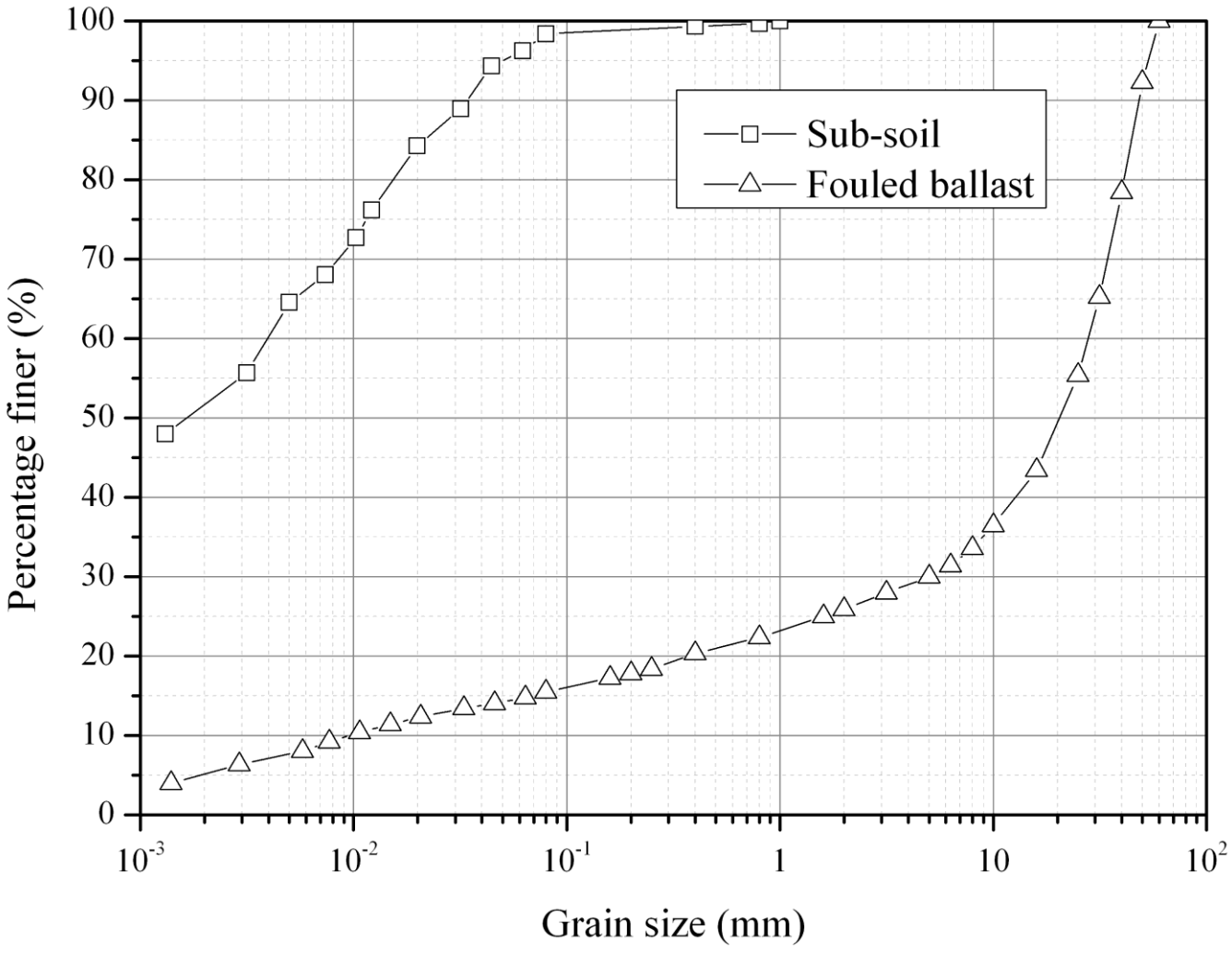

Figure 1. Grain size distributions of fouled ballast and sub-soil from the Sénissiat site

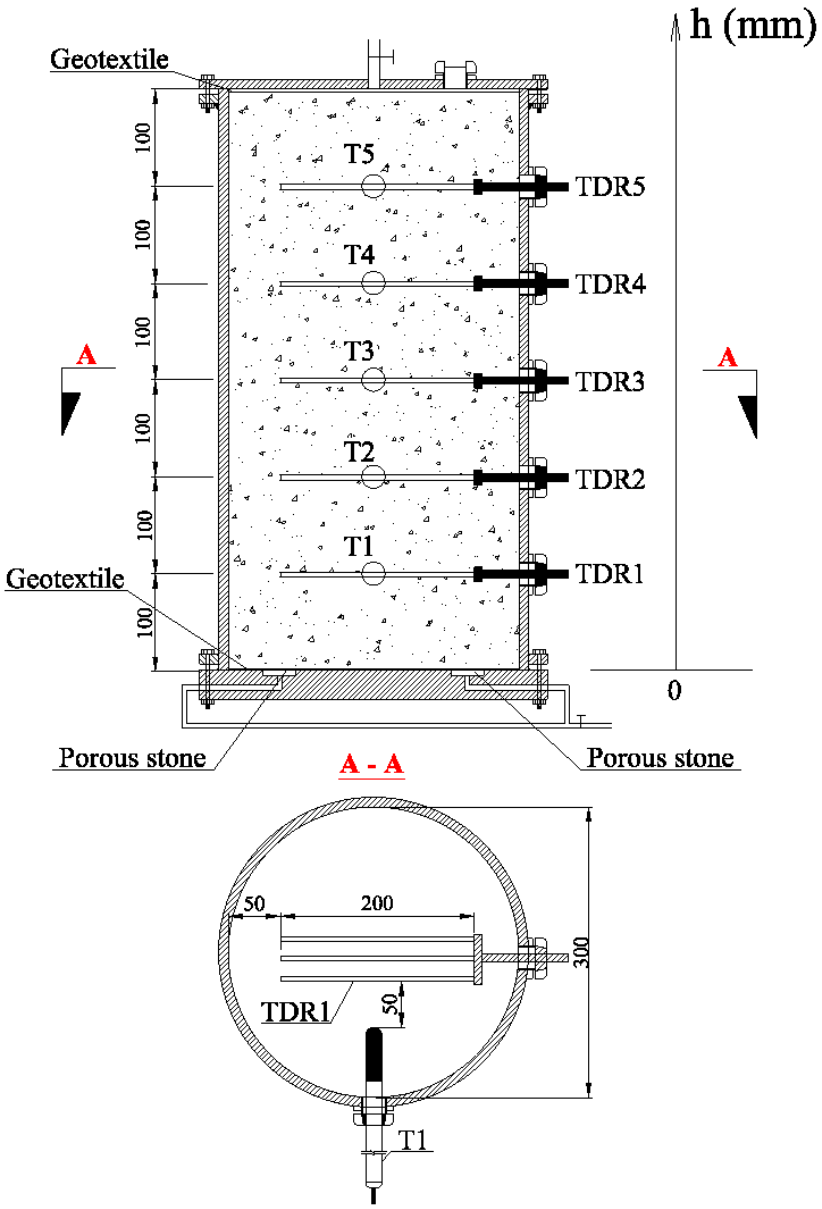

481

482 **Figure 2. Schematic view of the infiltration column**

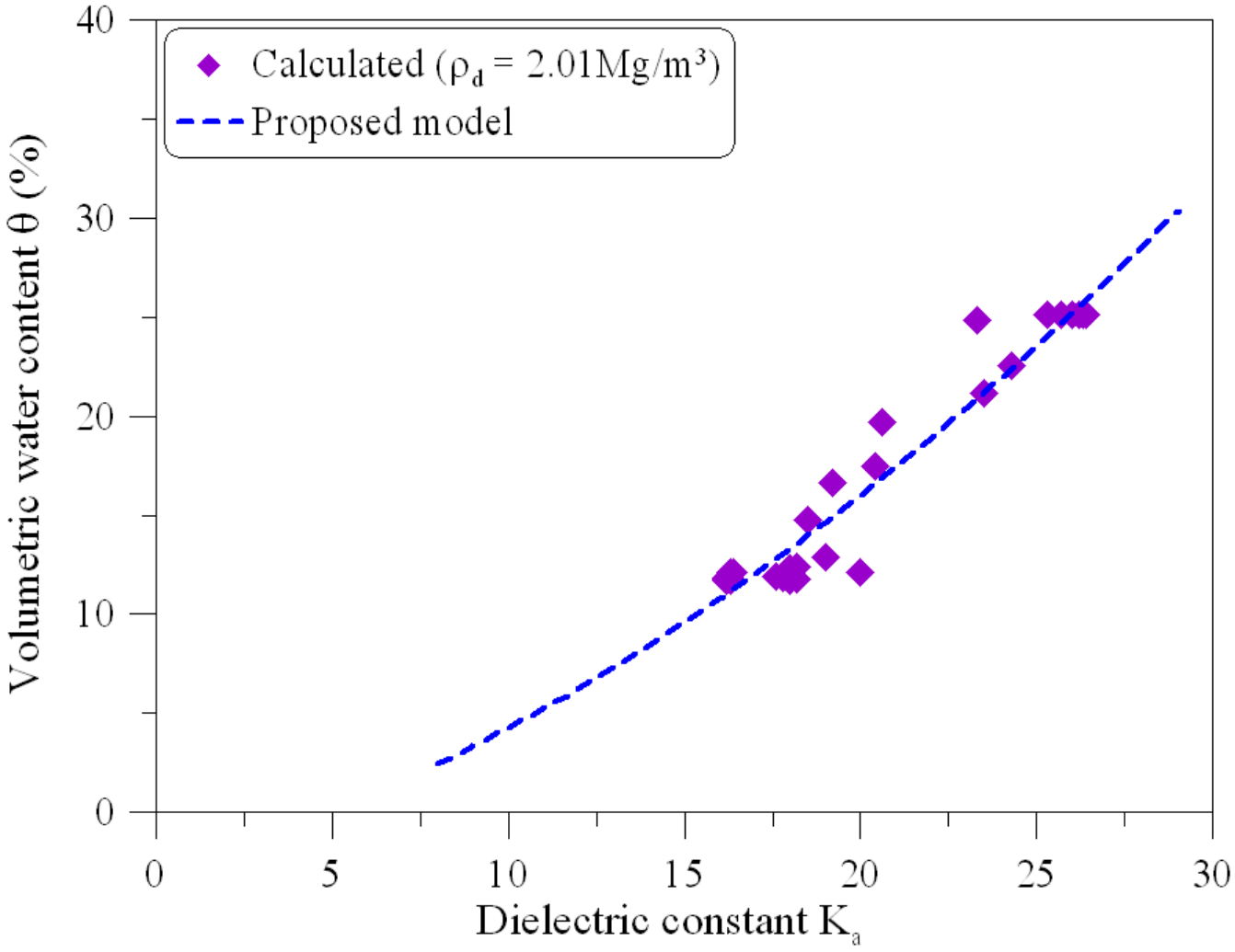

Figure 3: TDR calibration curve

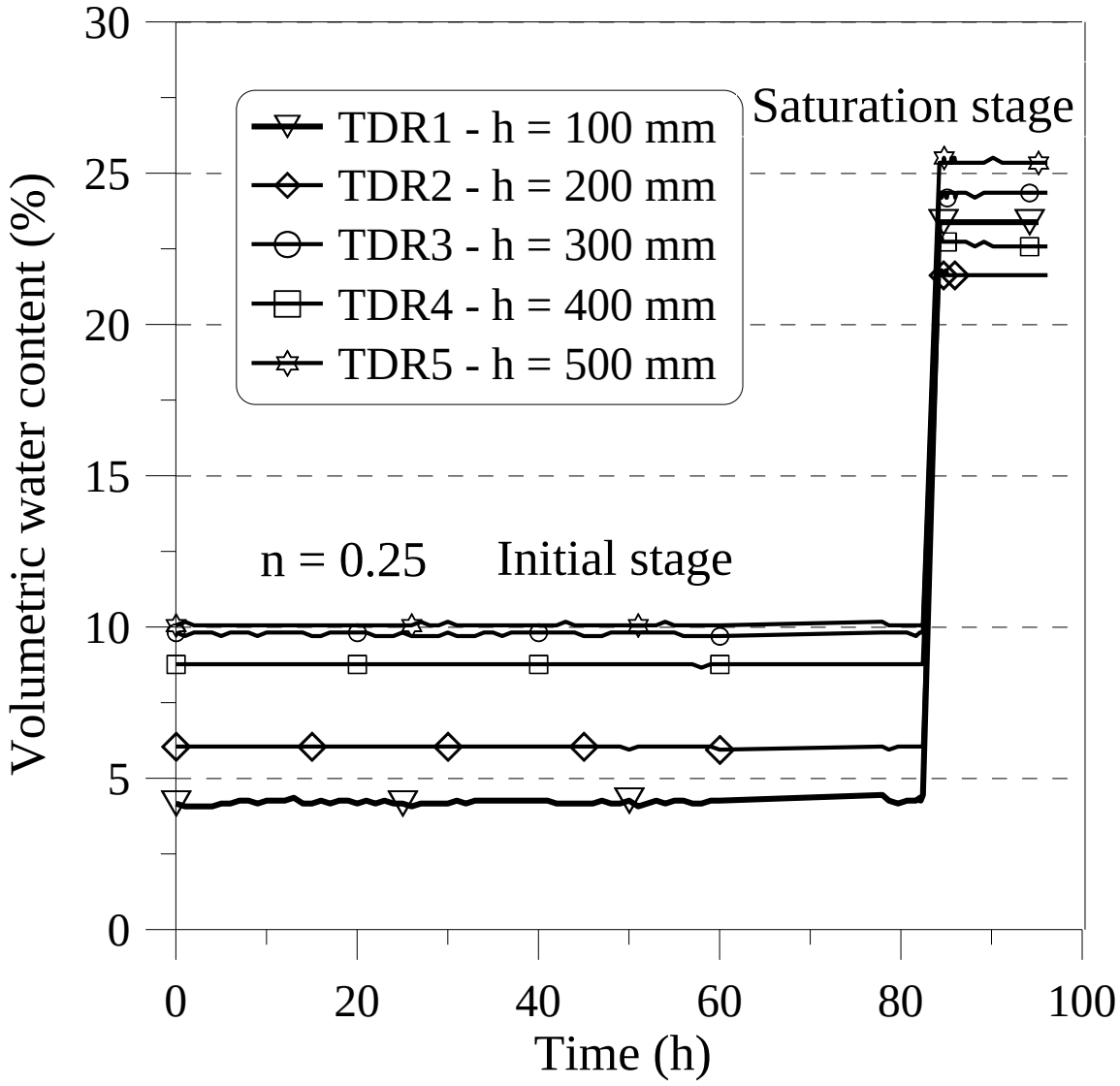

Figure 4. Volumetric water content – in the initial stage and in the saturation stage

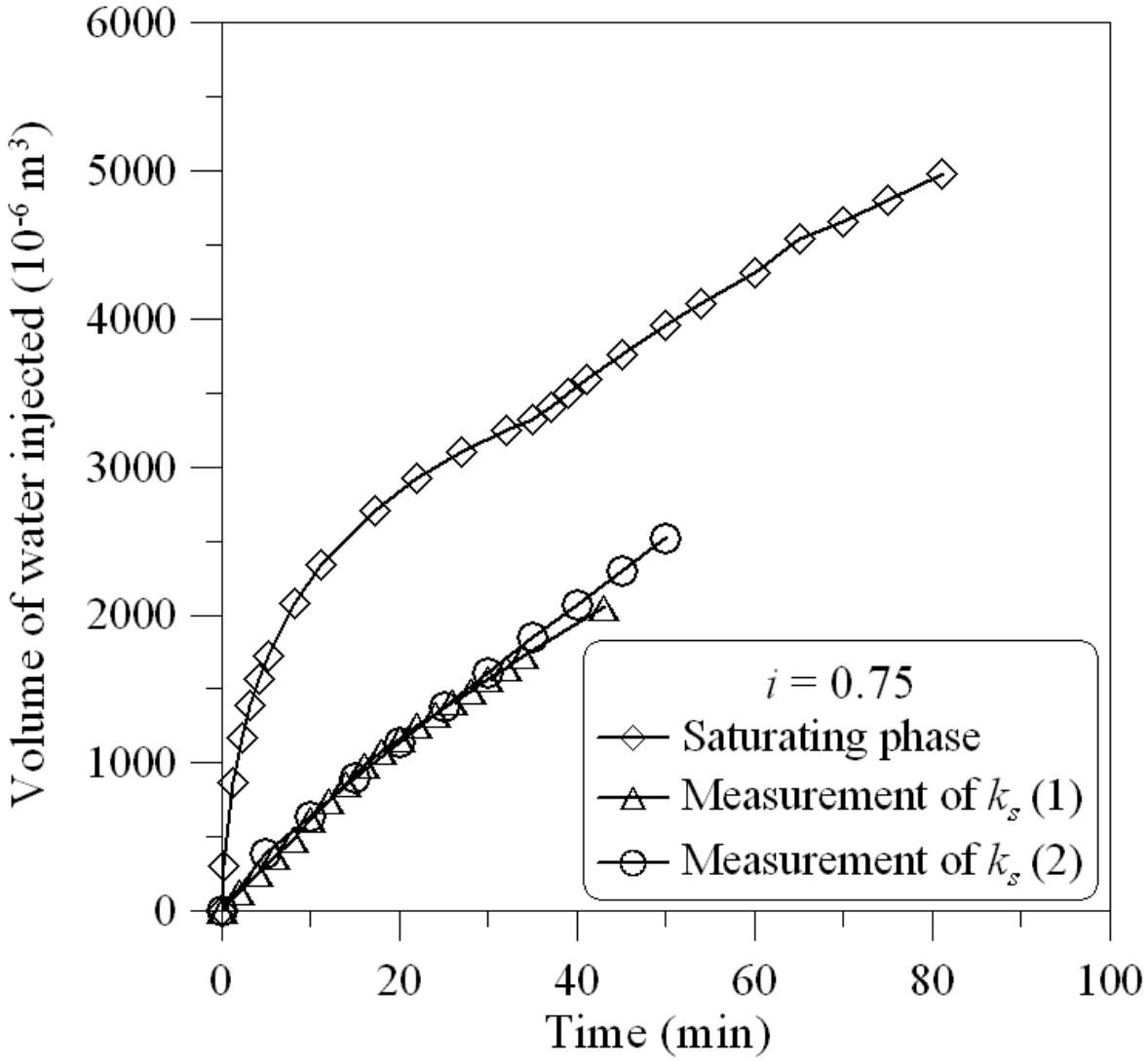

491
492 Figure 5. Water volume injected during saturation and hydraulic conductivity measurements

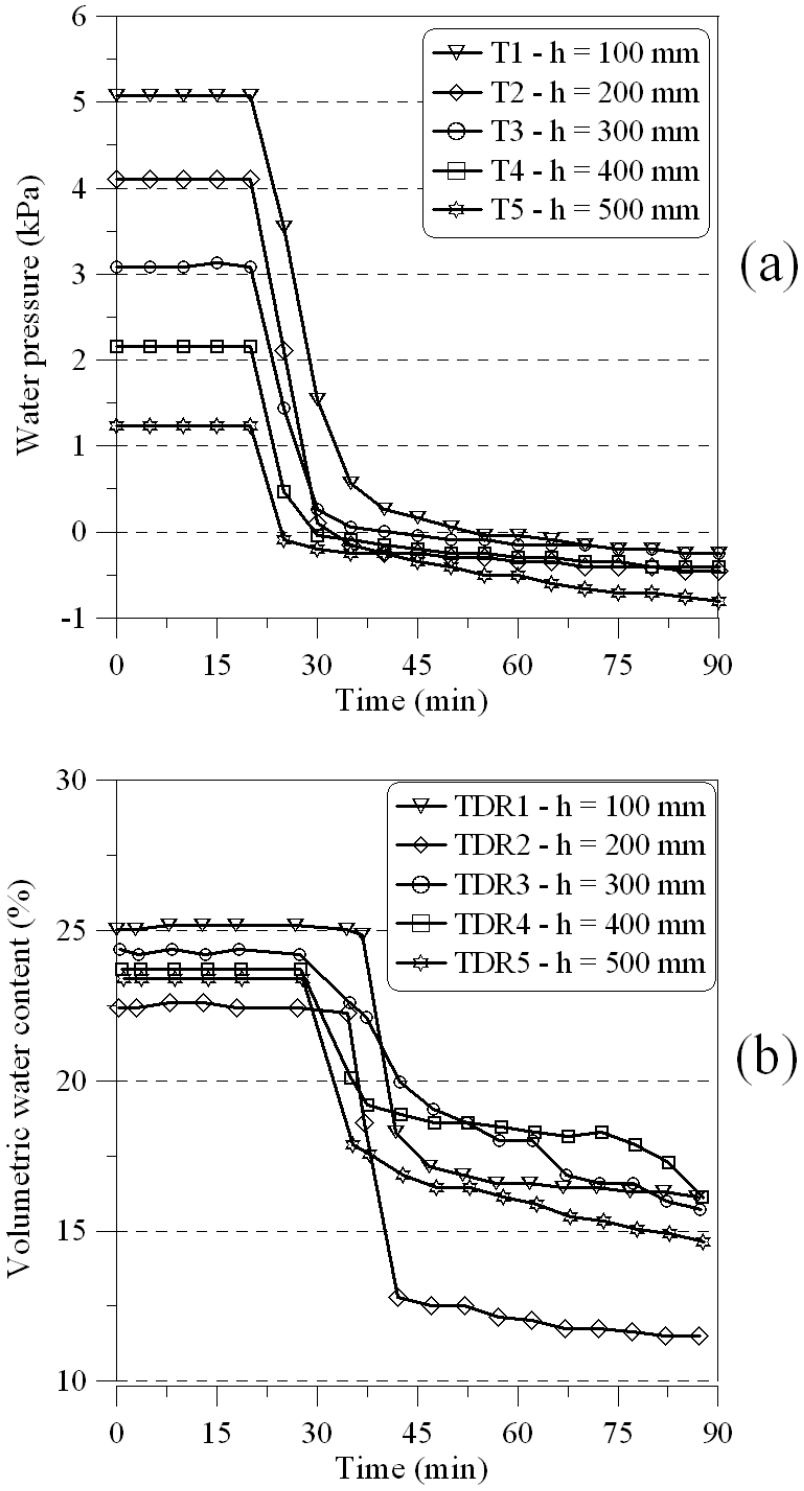

493

494 **Figure 6. Water pressure (a) and volumetric water content (b) evolution from 0 to 90 min – drainage stage**

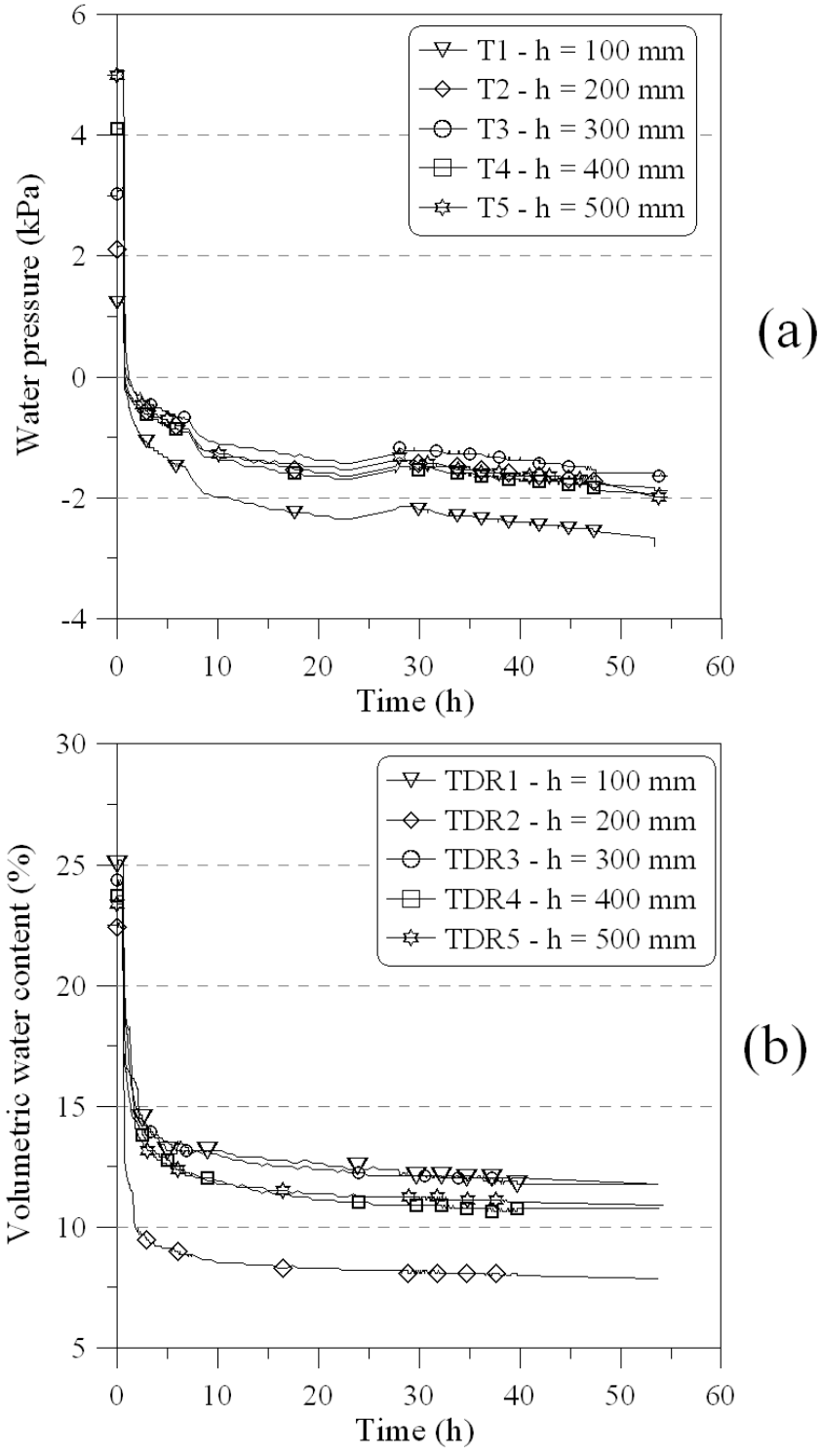

495

496 **Figure 7. Water pressure (a) and volumetric water content (b) evolution – drainage stage**

497

498

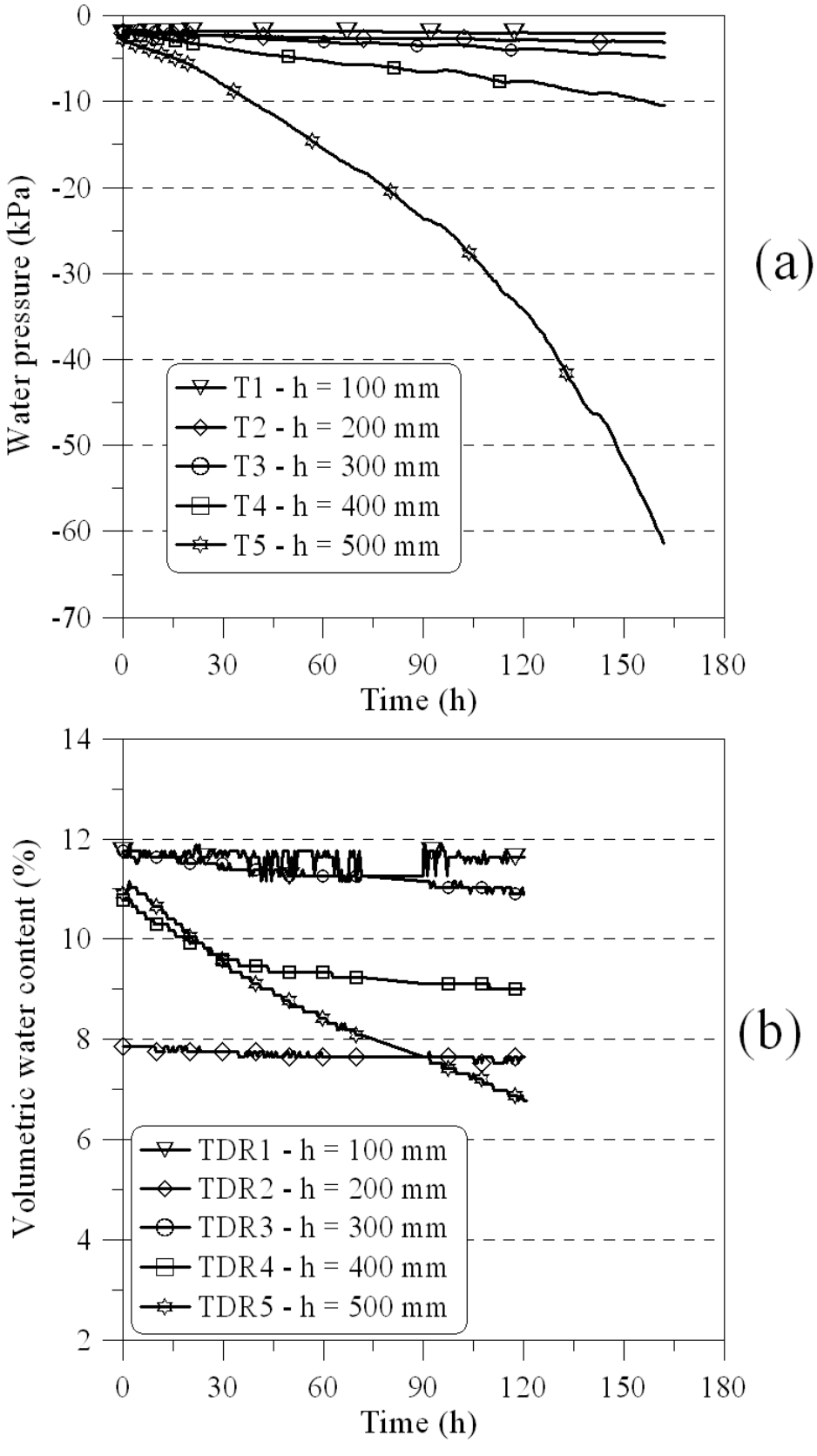

Figure 8. Water pressure (a) and volumetric water content (b) evolution – evaporation stage

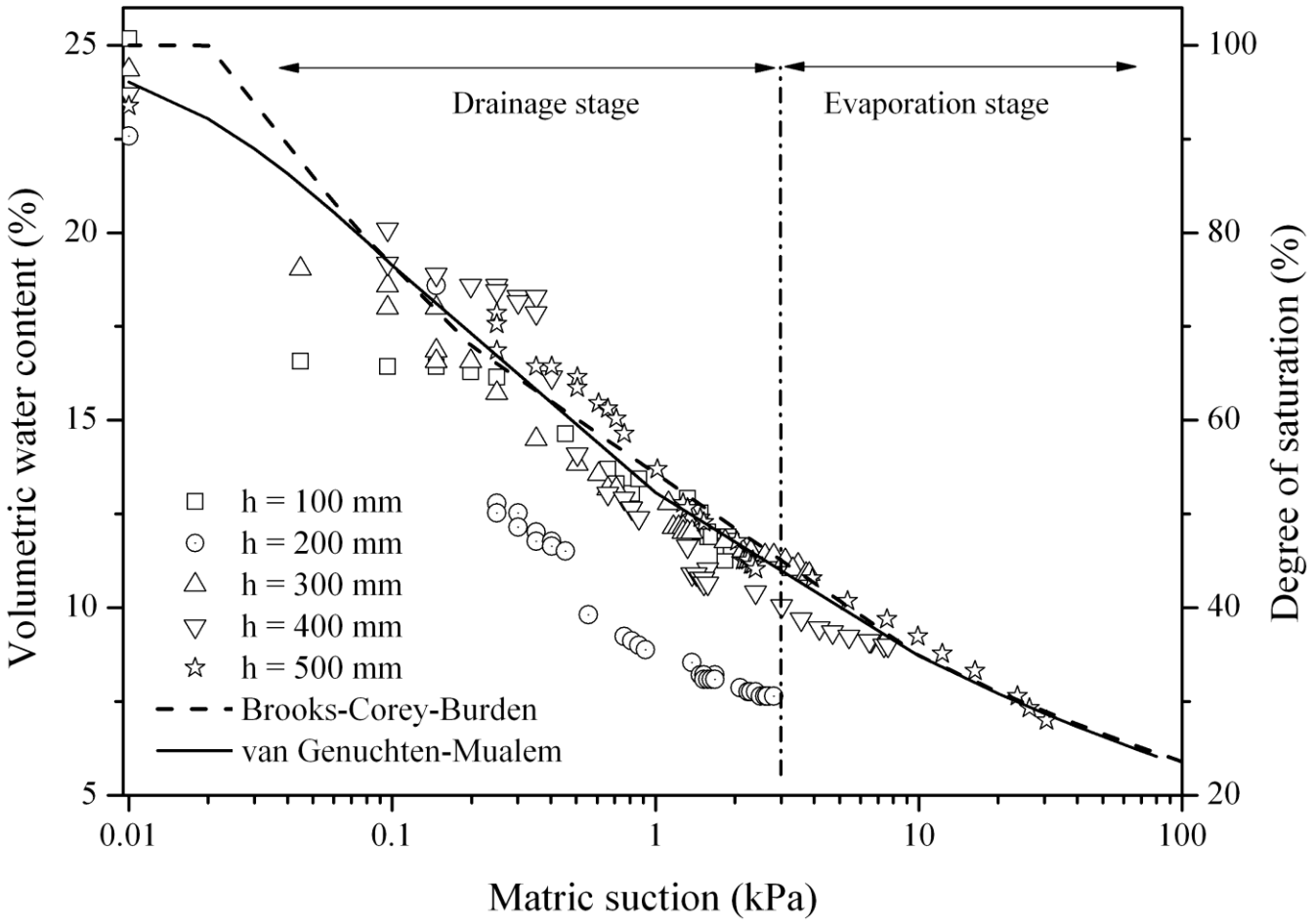

Figure 9. Measured water retention curves along with van Genuchten and Brooks-Corey water retention functions fitted to independent data

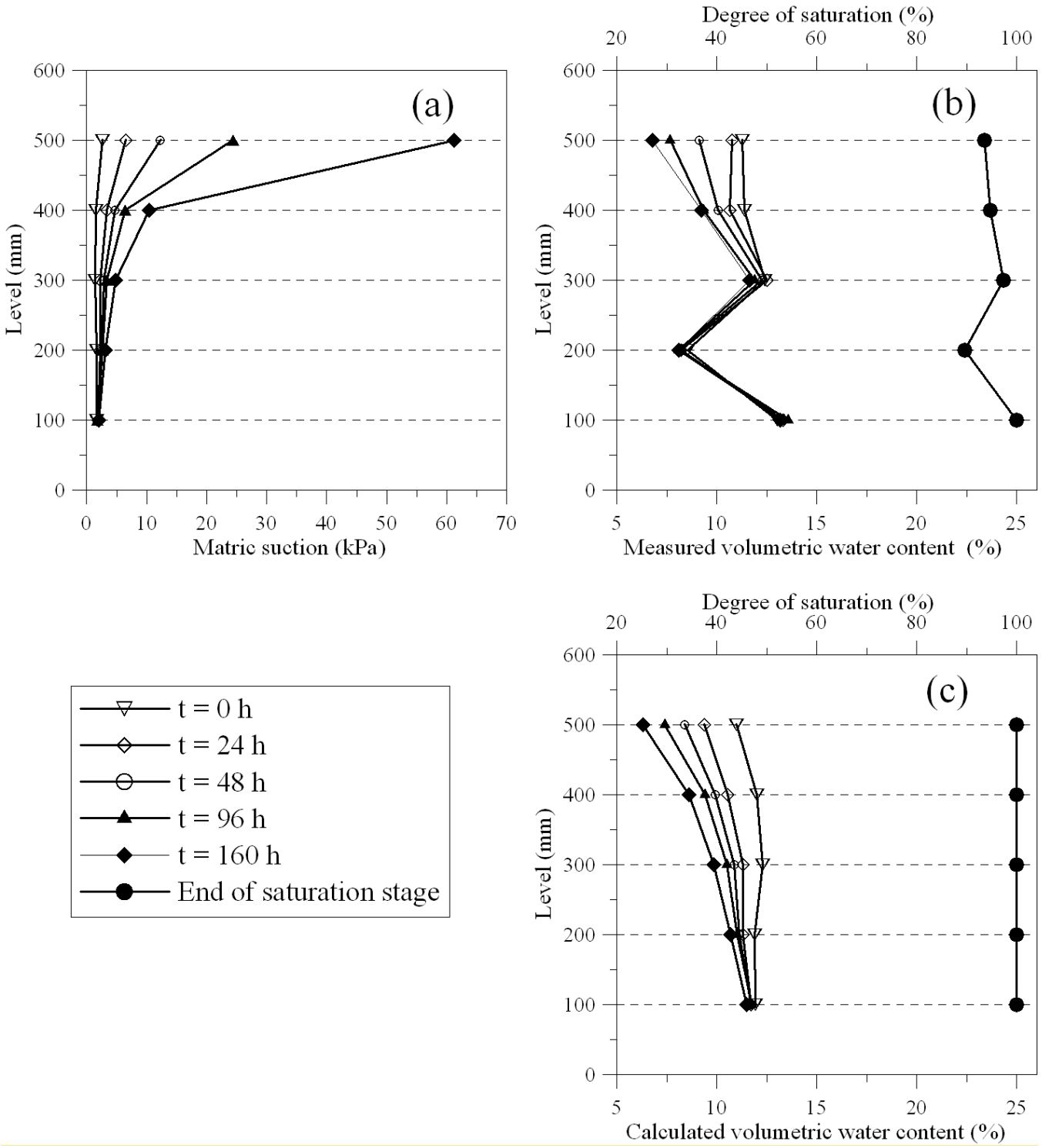

506

507 **Figure 10. Evolution of profiles. (a) suction; (b) measured volumetric water content; (c) volumetric water content by**
508 **van Genuchten's model**

509

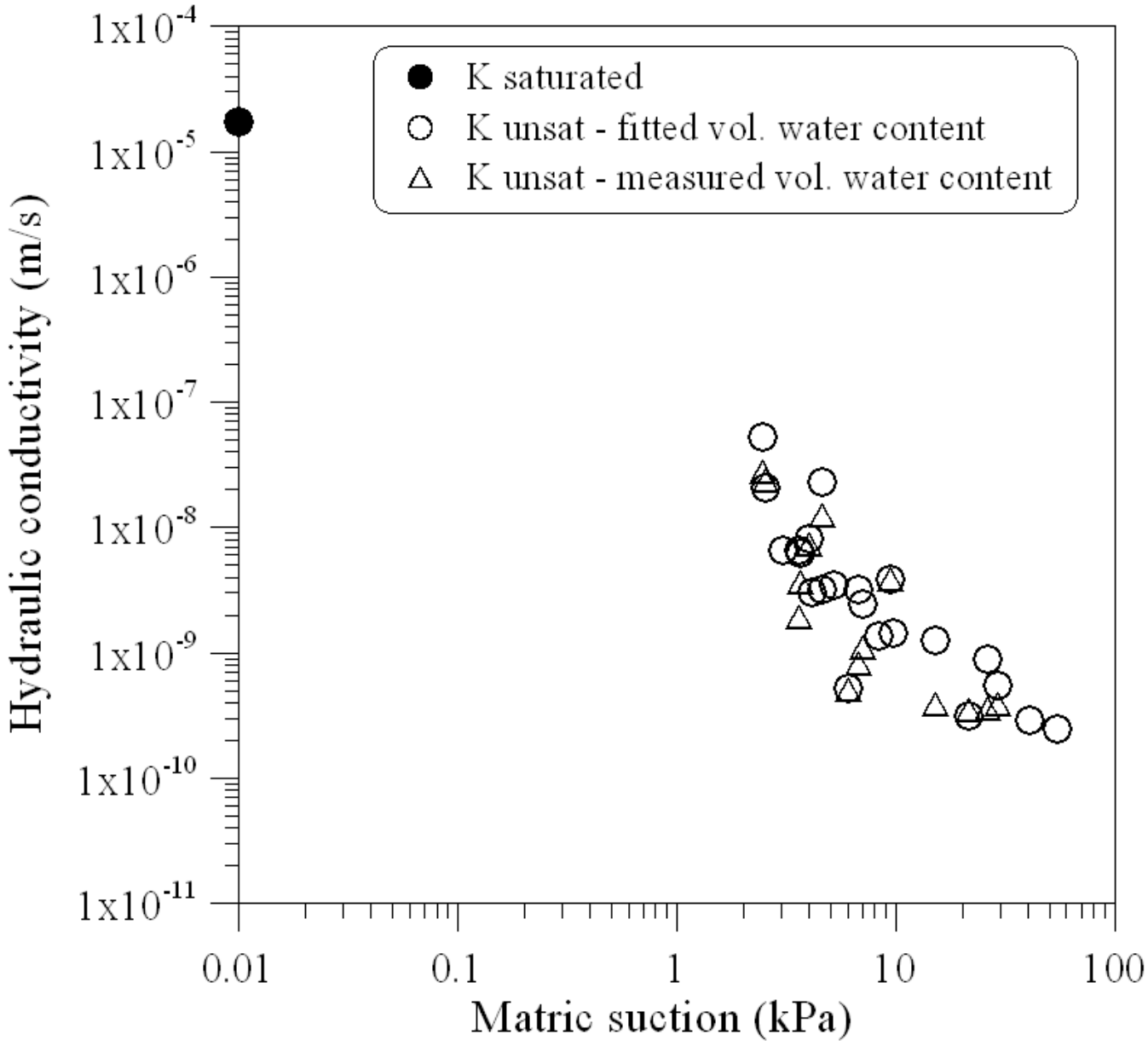

510

511 **Figure 11: Unsaturated hydraulic conductivity versus suction**

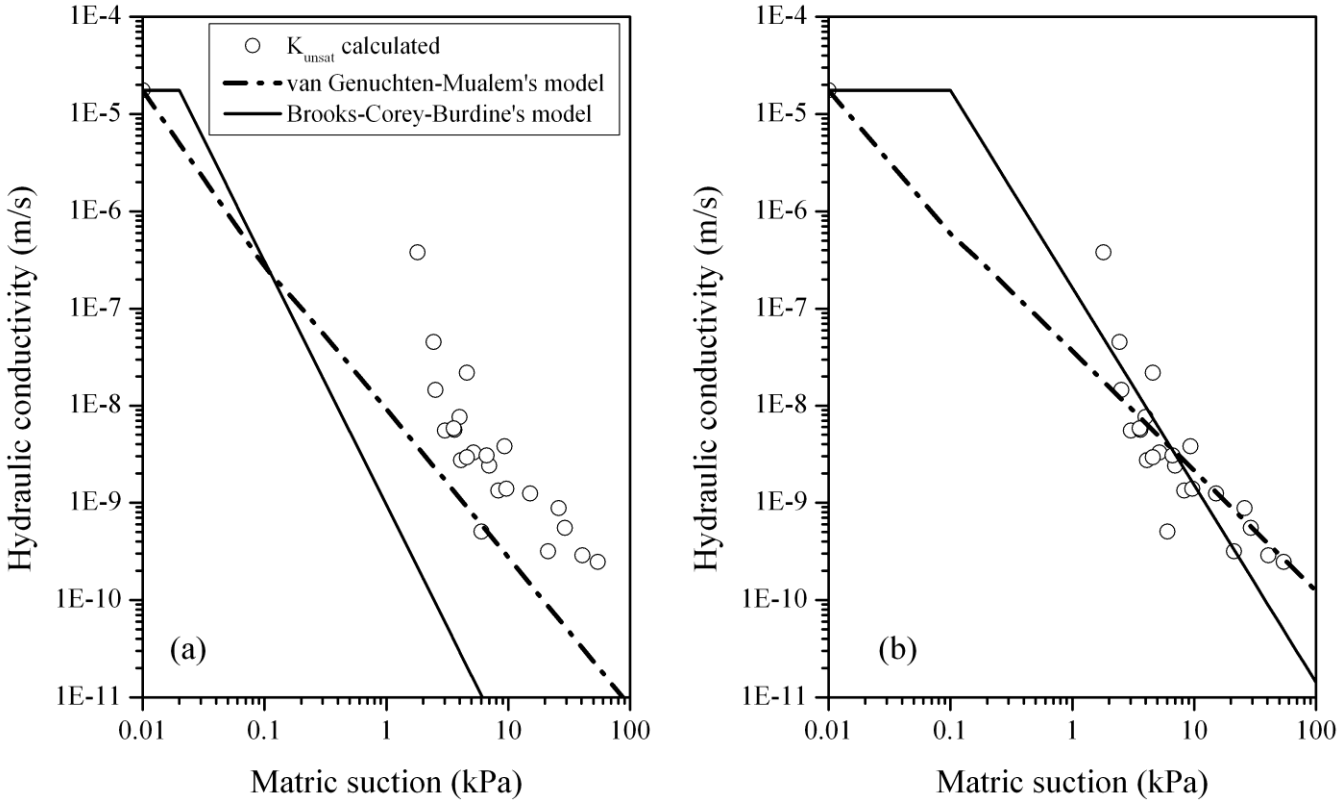

512

513 **Figure 12: Comparison between calculated hydraulic conductivity values with those predicted by the van Genuchten-**
514 **Mualem and Brooks-Corey-Burdine models. (a) before rectification and (b) after rectification**